Cardiovascular Research (2017) **113**, 183–194
doi:10.1093/cvr/cvw213

Attenuation of carotid neointimal formation after direct delivery of a recombinant adenovirus expressing glucagon-like peptide-1 in diabetic rats

Soo Lim[1,2], Gha Young Lee[1], Ho Seon Park[2], Dong-Hwa Lee[1,2], Oh Tae Jung[1,2], Kim Kyoung Min[1,2], Young-Bum Kim[3], Hee-Sook Jun[4], Jang Hak Chul[1,2], and Kyong Soo Park[2]*

[1]Department of Internal Medicine, Seoul National University Bundang Hospital, Seongnam, Korea; [2]Department of Internal Medicine, Seoul National University College of Medicine, Seoul, Korea; [3]Division of Endocrinology, Diabetes and Metabolism, Department of Medicine, Beth Israel Deaconess Medical Center and Harvard Medical School, Boston, MA, USA; and [4]Lee Gil Ya Cancer and Diabetes Institute, Department of Medicine, Gachon University of Medicine and Science, Incheon, Korea

Received 7 July 2016; revised 28 August 2016; editorial decision 21 September 2016; accepted 29 September 2016; online publish-ahead-of-print 4 October 2016

Time of primary review: 36 days

Aims Enhancement of glucagon-like peptide-1 (GLP-1) reduces glucose levels and preserves pancreatic β-cell function, but its effect against restenosis is unknown.

Methods and results We investigated the effect of subcutaneous injection of exenatide or local delivery of a recombinant adenovirus expressing GLP-1 (rAd-GLP-1) into carotid artery, in reducing the occurrence of restenosis following balloon injury. As a control, we inserted β-galactosidase cDNA in the same vector (rAd-βGAL). Otsuka Long-Evans Tokushima rats were assigned to three groups ($n = 12$ each): (1) normal saline plus rAd-βGAL delivery (NS + rAd-βGAL), (2) exenatide plus rAd-βGAL delivery (Exenatide + rAd-βGAL), and (3) normal saline plus rAd-GLP-1 delivery (NS + rAd-GLP-1). Normal saline or exenatide were administered subcutaneously from 1 week before to 2 weeks after carotid injury. After 3 weeks, the NS + rAd-βGAL group showed the highest intima–media ratio (IMR; 3.73 ± 0.90), the exenatide + rAd-βGAL treatment was the next highest (2.80 ± 0.51), and NS + rAd-GLP-1 treatment showed the lowest IMR (1.58 ± 0.48, $P < 0.05$ vs. others). The proliferation and migration of vascular smooth muscle cells and monocyte adhesion were decreased significantly after rAd-GLP-1 treatment, showing the same overall patterns as the IMR. In injured vessels, the apoptosis was greater and MMP2 expression was less in the NS + rAd-GLP-1 than in the exenatide or rAd-βGAL groups. *In vitro* expressions of matrix metalloproteinases-2 and monocyte chemoattractant protein-1 and nuclear factor-kappa-B-p65 translocation were decreased more in the NS + rAd-GLP-1 group than in the other two groups (all $P < 0.05$).

Conclusion Direct GLP-1 overexpression showed better protection against restenosis after balloon injury via suppression of vascular smooth muscle cell migration, increased apoptosis, and decreased inflammatory processes than systemic exenatide treatment. This has potential therapeutic implications for treating macrovascular complications in diabetes.

Keywords Glucagon like peptide-1 • Exenatide • Atherosclerosis • Inflammation • Apoptosis • Neointima

1. Introduction

Cardiovascular disease is the main cause of death in patients with type 2 diabetes (T2D). Almost 80% of such patients are believed to die from cardiovascular diseases such as myocardial infarction or stroke. Primary coronary intervention with stent implantation is now widely performed for patients with symptomatic coronary artery diseases. Although the development of drug-eluting stents has reduced the incidence of restenosis after coronary intervention, restenosis of the intervened vessel is still a critical issue of significant magnitude.[1]

* Corresponding author. Department of Internal Medicine, College of Medicine, Department of Molecular Medicine and Biopharmaceutical Sciences, Graduate School of Convergence Science and Technology, Seoul National University, Seoul, Korea. Tel: +82 2 2072 2946, E-mail: kspark@snu.ac.kr

It is now known that glucagon like peptide-1 (GLP-1) treatment improves cardiac function in cases of heart failure or after acute myocardial infarction. In a rat model of chronic heart failure, 11 weeks of treatment with GLP-1 improved the left ventricular (LV) ejection fraction and end diastolic pressure.[2] Activation of the GLP-1 receptor with GLP-1 significantly mitigated myocardial injury in a study using isolated perfused rat hearts.[3] Furthermore, in dogs with dilated cardiomyopathy induced by excessive pacing, the stimulation of GLP signalling with GLP-1 improved their cardiac performance.[4] In human patients with acute myocardial ischemia, a GLP-1 infusion improved regional and global cardiac functions.[5] In a recent large clinical trial, the rate of the first occurrence of death from cardiovascular causes, non-fatal myocardial infarction, or non-fatal stroke among patients with T2D was lower with liraglutide than with placebo.[6] In this context, it would be interesting to investigate whether activation of the GLP-1 receptor has a role in preventing restenosis after vascular injury, and more generally has potential anti-atherosclerotic properties.

We have shown that the continuous expression of GLP-1 *in vivo* regenerates pancreatic β-cells and improves glucose homeostasis in mice, using an adenoviral vector containing the cytomegalovirus promoter/enhancer and albumin leader sequence followed by the GLP-1 cDNA sequence (rAd-GLP-1).[7] Here, we investigated the effect of direct rAd-GLP-1 delivery to injured vessels, and systemic injection of exenatide, a GLP-1 agonist, in reducing the occurrence of restenosis after a vascular balloon injury in an animal model of insulin resistance.

Among many factors, the expression and activity of matrix metalloproteinases (MMPs) have been reported to correlate with the macrovascular complications of diabetes.[8,9] Nuclear factor-kappa-B (NF-κB), a core mediator in the inflammatory cascade, is activated in the milieu of atherosclerosis and insulin resistance. Therefore, we investigated alterations in MMPs and NF-κB levels after treatment using injured vessels obtained from the study animals, and in vascular cell lines to elucidate possible related mechanisms.

2. Methods

2.1 Construction of a recombinant adenovirus expressing GLP-1 (rAd-GLP-1)

We constructed a recombinant adenoviral vector containing the CMV promoter/enhancer and albumin leader sequence (25 amino acids) followed by the GLP-1 cDNA sequence (amino acids 7–37), which encodes active GLP-1 (rAd-GLP-1). As a control, we replaced the albumin leader-GLP-1 cDNA with the β-galactosidase cDNA in the same vector (rAd-βGAL). The expression of GLP-1 by the rAd-GLP-1 vector was confirmed by reverse transcriptase–polymerase chain reaction (RT–PCR) using an immortalized human hepatocyte line.[10] Briefly, expression of GLP-1 mRNA was first detected at 8 h after rAd-GLP-1 infection and increased further by 24 h, whereas GLP-1 mRNA was not detected in rAd-βGAL-infected cells.[7]

2.2 Study animals and care

Thirty-six Otsuka Long-Evans Tokushima Fatty (OLETF) rats (4 weeks old, male), the animal model for obese T2D, were donated by Japanese Otsuka Pharmaceuticals (Otsuka Holdings Co., Ltd., Tokyo, Japan). OLETF rats naturally develop T2D around 24 weeks of age and have been used in studies investigating glucose metabolism and cardiovascular complications in this condition.[11] After being raised in plastic cages in an air-conditioned room at 22 ± 2 °C and 55 ± 10% humidity for 24 weeks, 28 week-old rats weighing 500–600 g were studied. The animals were all allowed free access to water and regular chow diet (Purina Korea, Seoul, South Korea), and diet and water consumption were recorded once a week. Animals were weighed twice a week at the same time in the morning.

Rats were placed into three groups: (1) normal saline subcutaneous (SC) injection + rAd-βGAL delivery (NS + rAd-βGAL) as a control, (2) exenatide SC injection + rAd-βGAL delivery (Exenatide + rAd-βGAL), and (3) normal saline (NS) SC injection + rAd-GLP-1 delivery (NS + rAd-GLP-1) ($n = 12$ per group). Exenatide (0.5 μg/kg) or normal saline was administered twice from 1 week before to 2 weeks after carotid injury.

Animal experiments were performed in compliance with the Guide for Experimental Animal Research of the Laboratory for Experimental Animal Research, Clinical Research Institute, Seoul National University Bundang Hospital, Republic of Korea. All animal procedures were performed to conform with the National Institutes of Health guidelines.

2.3 Animal studies

2.3.1 Rat carotid artery balloon denudation injury

A previously well-established rat carotid artery balloon injury model was used in this study.[12] Rats were anesthetized with a combination of anaesthetics (ketamine, 70 mg/kg; xylazine, 7 mg/kg IP; Yuhan Corp, Seoul, South Korea). After the left external carotid artery was exposed, heparin (30 IU) was administered systemically via the external jugular vein. A 2F Fogarty embolectomy catheter (Baxter Healthcare Corp, IL, USA) was introduced into an external carotid arteriotomy incision, advanced to the common carotid artery, and inflated with 0.2–0.25 mL of normal saline and withdrawn 10 times with rotation. After clamping both the common carotid and the internal carotid arteries proximally, mixtures containing 5×10^8 pfu of adenovirus containing either rAd-GLP-1 or rAd-βGAL diluted to a total volume of 100 μL were instilled via the arterial segment between the two clamps.[13] Clamping of the artery was released at 20 min after instillation.

2.3.2 Morphometric analysis

Two weeks after balloon injury, rats were euthanized with a lethal dose of pentobarbital (150 mg/kg), and carotid arteries were fixed by perfusion at 120 mmHg with 4% formaldehyde via an 18G intravenous cannula placed retrograde in the abdominal aorta. Tissues were then embedded in paraffin, and sections were stained with H&E. The extent of neointimal formation in histologically stained sections was quantified by computed planimetry. The cross-sectional areas of the blood vessel layers, i.e. the lumen, intimal, and medial areas, are quantified in 3 different sections (proximal, middle, and distal) using an Image-Pro® Plus Analyser Version 4.5 (Media Cybernetics, Silver Spring, MD, USA). The intima-media ratio (IMR) was calculated from the mean of these determinations.

2.3.3 Immunoblot analysis of GLP-1 receptors in carotid arteries

Harvested vessel tissues were homogenized with cell lysis buffer (Cell Signalling, Danvers, MA, USA) containing 20 mM Tris (pH 7.5), 150 mM NaCl, 1 mM Na_2EDTA, 1% Triton, 2.5 mM sodium pyrophosphate, 1 mM β-glycerophosphate, 1 mM Na_3VO_4, 1 mg/ml leupeptin, and 1 mM phenylmethylsulfonyl fluoride for 30 min at 4 °C, and protein lysate concentrations were measured using Bradford protein assay kits (BioRad, Hercules, CA, USA). The same amounts of proteins from whole cell lysates were subjected to sodium dodecyl sulfate polyacrylamide gel

electrophoresis and transferred onto methanol-treated polyvinylidene difluoride membranes (Millipore Co., Bedford, MA, USA). After blocking the membrane with Tris-buffered saline with Tween 20 (TBS-T) containing 5% blocking buffer for 1 h at room temperature, they were washed with TBS-T and incubated with primary antibodies against GLP-1 receptor (Santa Cruz Biochemicals, Dallas, TX, USA) or γ-tubulin (Sigma Aldrich, St Louis, MO, USA) for 1 h at room temperature or overnight at 4 °C. The membranes were washed three times with TBS-T for 10 min and then incubated for 1 h at room temperature with horseradish peroxidase-conjugated secondary antibodies. After washing, the bands were detected using enhanced chemiluminescence reagents (Santa Cruz Biochemicals).

2.3.4 Immunohistochemical staining for proliferation and apoptosis

To determine whether exenatide injection or rAd-GLP-1 delivery could affect cell proliferation directly, we measured cell proliferation by immunostaining for proliferating cell nuclear antigen (PCNA) in the tissue sections of injured arteries. Briefly, deparaffinized specimens were treated with protease K for 4 min, and endogenous peroxidase was then quenched with a methanol/peroxidase solution. The specimens were treated with 50 mmol/L Tris HCl (pH 7.6) containing 0.15 mol/L NaCl and 0.1% Tween 20 for 5 min, and then incubated in 1:50 diluted anti-PC-10 antibody (Dako, Cincinnati, OH, USA). The specimens were then incubated with 1:50 diluted 3,39-diaminobenzidine tetrahydrochloride substrate solution and counterstained with Mayer hematoxylin (Dako). Proliferation was defined as the percentage of PCNA-positive cells among the total number of nucleated cells in four fields per tissue section.

To examine the effects of exenatide injection or rAd-GLP-1 delivery on apoptosis after balloon injury *in vivo*, we performed terminal deoxynucleotidyl transferase dUTP nick end labelling (TUNEL) staining in the tissue sections of injured arteries.[14] Briefly, 5 μm sections were deparaffinized and incubated with proteinase K (Dako) (20 μg/mL) for 15 min at room temperature. An apoptosis detection kit (Apoptag, Intergen Col, Purchase, NY, USA) was used with the chromogen 3,3'-diaminobenzidine. Counterstaining was applied with Mayor hematoxylin (Dako). Apoptotic cells were quantified by calculating the percentages of TUNEL-positive cells over total nucleated cell counts in four fields per tissue section.

2.3.5 Immunohistochemical staining of CD68 for monocytes and CD31 for endothelial cells

For immunohistochemistry of CD68 and CD31, sections were rehydrated, blocked with 5% goat serum and 0.01% Triton X-100 in PBS, and incubated with the monocyte/macrophage marker anti-CD68 (Abcam, Cambridge, MA, USA) or the endothelial cell marker anti-CD31 (AbD Serotec, Kidlington, UK) for 1 h. After they had been rinsed with PBS, horseradish peroxidase-conjugated antibody to rabbit IgG or mouse IgG was applied for 20 min. Sections were exposed for 4 min to 0.04% diaminobenzidine tetrahydrochloride (DAB) in 0.05 mol/L Tris-maleate buffer (pH 7.6) with 0.006% H_2O_2 and counterstained with hematoxylin.

2.3.6 Biochemical markers associated with cardiovascular risk

An intraperitoneal glucose tolerance test (IPGTT) was performed at baseline and 3 weeks after exenatide or normal saline injections. After the 10 h fasting glucose concentration had been measured, each animal was injected intraperitoneally with 1.5 g/kg of a 1 mol/L glucose solution. Blood samples (about 10 μL) were collected from the tail at 30, 60, and 120 min after the glucose load. Plasma glucose concentration was measured using reagent strips read in a glucose meter (YSI 2300-STAT, Yellow Springs, OH, USA). The homeostasis model assessment of the insulin resistance (HOMA-IR) and pancreatic β-cell function (HOMA-β) were calculated using fasting insulin and glucose concentrations.[15] In addition, the area under the curve of glucose ($AUC_{glucose}$) was calculated using the trapezoid method from the IPGTT glucose values measured at 0–120 min.

Serum high-sensitivity C-reactive protein (hsCRP) and adiponectin levels were measured using rat-specific enzyme-linked immunosorbent assay kits (BD Biosciences Pharmingen, Heidelberg, Germany and AdipoGen Co., Seoul, Republic of Korea, respectively). Tumour necrosis factor (TNF)-α, interleukin (IL)-6, plasminogen activator inhibitor-1 (PAI-1) activity, and monocyte chemoattractant protein-1 (MCP-1) levels were measured using the RADPK-81K kit (Linco, Billerica, MA, USA).

2.4 Cell studies

Rat aortic smooth muscle cells (RAoSMCs) were purchased from Bio-Bud (Seoul, Republic of Korea) and cultured in Dulbecco's modified Eagle's medium (DMEM) (Gibco BRL, Grand Island, NY, USA) supplemented with 100 U/mL penicillin-streptomycin, and 10% foetal bovine serum (FBS). Human umbilical vein endothelial cells (HUVECs; Cambrex, Walkersville, MD, USA) were cultured in endothelial cell growth medium (EGM-2) (Cambrex) containing 2% FBS, 0.4% hydrocortisone, 0.1% VEGF, 4% hFGF-B, 0.1% R3-IGF, 0.1% hEGF, 0.1% ascorbic acid, 0.1% GA-1000, and 0.1% heparin, according to the manufacturer's instructions. The RAoSMCs and HUVECs were obtained from the same batches, respectively and cells at 3–6 passages were used. RAoSMCs were starved for 48 h before use, and HUVECs were starved in endothelial cell basal medium (EBM-2; Cambrex) supplemented with 0.2% FBS for 24 h. We repeated all cell studies five times.

2.4.1 Expression of the GLP-1 receptor in RAoSMCs after exenatide or rAd-GLP-1 treatments

To investigate the expression level of the GLP-1 receptor, starved RAoSMCs were treated with various doses (0, 5, 10, 20, or 40 nM) or durations (0, 3, 6, 12, 24, or 48 h) of exenatide. The cells were harvested and were solubilized in cell lysis buffer (Cell Signalling). Protein lysates were subjected to western blotting using an anti-GLP-1 receptor antibody (Santa Cruz Biotechnology).

2.4.1.1 Cell proliferation. Cell proliferation was determined using a modified 3-(4,5-dimethyl-thiazol-2-yl)-2,5-diphenyltetrazolium bromide (MTT) assay; 5 mg/mL of MTT was dissolved in phosphate-buffered saline (PBS). RAoSMCs were grown in 48-well plates at a density of 2×10^3 per well starved for 48 h as above, and then placed in DMEM supplemented with 0.5% FBS. The cells were exposed to exenatide (10 nM), rAd-GLP-1 at 5 and 10 multiplicities of infection (MOI), and rAd-βGAL at 10 MOI for 24 h. For platelet-derived growth factor-subunit B (PDGF-BB) stimulation, cells were incubated with 10 ng/mL of PDGF-BB (R&D Systems, Camarillo, USA) for an additional 24 h. Then, a 200 μL aliquot from each well was transferred to a 96-well plate, and light absorbance was measured at 570 nm using a spectrophotometer.

2.4.2 Expression of p27 in RAoSMCs

To measure the expression level of p27, a cell cycle inhibitor protein, starved RAoSMCs were treated with exenatide, rAd-GLP-1, or

rAd-βGAL for 24 h prior to the addition of 10 ng/mL PDGF. The cells were harvested for 24 h after PDGF treatment and were solubilized in cell lysis buffer (Cell Signalling). Protein lysates were subjected to western blotting using an anti-p27 antibody (Cell Signalling).

2.4.3 Analysis of cellular apoptosis by flow cytometry

Starved RAoSMCs were treated with exenatide (10 nM), with rAd-GLP-1 at 5 and 10 MOI, and rAd-βGAL at 10 MOI for 24 h. The cells were harvested, washed with PBS, and fixed in cold 70% ethanol for at least 1 h, and then the cells were stained with 50 μg/mL propidium iodide for 15 min at 37 °C. A total of 1×10^4 cells were analysed using a FACScan flow cytometer (Becton Dickson, Franklin Lakes, NJ, USA). The percentages of cells in the apoptotic sub-G1 phase were calculated from the FACScan data.

2.4.4 Cell migration assessed by a wound-healing assay

RAoSMCs were grown to confluence in six-well plates and then starved in DMEM with 0.5% FBS for 48 h. Each well was divided into a 2 × 3 grid. Using a 1000 μL pipette tip, a linear wound was made in each hemisphere of the well. Immediately after wounding, the cells were incubated with 10 ng/mL of PDGF-BB (R&D systems) and were allowed to migrate for 24 h at 37 °C. Images were taken around the linear wound. The distance from the line of wounding to the point of maximum cell growth was measured from three fields per well.

2.4.5 Monocyte adhesion assay

To investigate effect of rAD-GLP-1 delivery and exenatide treatment on monocyte adhesion, primary rat monocytes were freshly isolated as previously described with slight modifications.[16] In brief, bone marrow cells from rats were separated using Ficoll and Percoll double gradient centrifugation (GE Healthcare, Buckinghamshire, UK). Fluorescence-labelled rat monocytes were washed three times with serum-free RPMI medium and then resuspended in the same medium. The cells (2×10^4) were added to the HUVEC monolayers, stimulated with TNF-α (10 ng/mL) for 18 h, and incubated for 30 min at 37 °C in 5% CO_2 in humidified air. Unbound cells were removed by washing three times with PBS. After being cultured in EBM-2 medium for 24 h, the rat monocytes adhering to endothelial cells were counted in three randomly selected fields of view in each well using microscopy

2.4.6 Western blotting analysis of NF-κB-p65 translocation

Because activation of the NF-κB signalling pathway induces the expression of adhesion molecules in endothelial cells, we investigated the effect of exenatide or rAd-GLP-1 treatment on the nuclear translocation of NF-κB. For this, the HUVECs were pretreated with 10 nM exenatide or infected with rAd-GLP-1 at 10 MOI for 24 h and then stimulated with 20 ng/mL of TNF-α for 15–30 min. Both nuclear and cytosolic fractions were subjected to western blotting using anti-p65 (Santa Cruz Biotechnology) and anti-phospho-IκB (Cell Signalling) antibodies.

2.4.7 MMP2 expression in RAoSMCs and HUVECs

The cells were pretreated with 10 nM exenatide or infected with rAd-GLP-1 at 5 or 10 MOI, and then stimulated with 10 ng/mL of TNF-α for 24 h. Total RNA was isolated from cells using TRIzol reagent (Invitrogen Life Technologies), and RT-PCR was performed according to the manufacturer's instructions. Based on GenBank searching (http://www.ncbi.nlm.nih.gov/genbank/), the RT–PCR primers were designed as follows: MMP-2 sense, 5'–ACCTGTCACTCCGGAGATCTGCAA–3' and antisense, 5'–TCACGCTCTTGAGACTTTGGTTCT–3'. The PCR conditions were: 30 cycles of 94 °C for 30 s, 55 °C for 30 s, and 72 °C for 45 s. The amplified products were visualized using 1.5% agarose gel electrophoresis and stained with ethidium bromide, and images were then captured under ultraviolet light. Densitometric analysis of the different observations was performed using Quantity One Software (Bio-Rad). The quantity of each transcript was normalized against GAPDH.

The effect of exenatide or rAd-GLP-1 treatment on MMP2 expression was also examined in HUVECs. Harvested cells were solubilized in cell lysis buffer (Cell Signalling). Protein lysate concentrations were measured using a Bradford protein assay kit (BioRad). A primary antibody for MMP2 (Santa Cruz) was applied.

2.4.8 MCP-1 and vascular cell adhesion molecule (VCAM) expression measured by RT-PCR

U937 cells and RAoSMCs were pretreated with 10 nM exenatide or infected with rAd-GLP-1 at 10 MOI and then stimulated with 10 ng/mL of TNF-α for 24 h. Total RNA was isolated, and RT–PCR was performed using gene-specific primers for MCP-1: sense, 5'–CTCGCTCAGCCAGATGCAATCAAT–3' and antisense, 5'–CCCAGGGGTAGAACTGTGGTTCAA–3' and VCAM, sense, 5'–ACACCTCCCCCAAGAATACAG–3', and antisense, 5'–GCTCATCCTCAACACCCACAG-3'. PCR products were analysed using agarose gel electrophoresis and visualized using ethidium bromide.

2.5 Statistical analysis

Results are reported as the mean ± standard deviation (SD). The Kolmogorov–Smirnov Goodness of Fit test was used to confirm the normal distribution of key variables. Skewed data distributions such as those for HOMA-IR, HOMA-β, and hsCRP were normalized by logarithmic transformation before all analyses. Mean values were compared for each treatment group by analysis of variance with least significant difference *t* tests. Analysis was done using IBS SPSS statistics for Windows (version 18.0; IBM Corp., Armonk, NY, USA). For all tests, $P < 0.05$ was considered to be statistically significant.

3. Results

3.1 Animal studies

3.1.1 GLP-1 receptor expression in carotid arteries

Expression of the GLP-1 receptor was confirmed by western blotting of the harvested vessel tissues (see Supplementary material online, *Figure S1*). The expression of GLP-1 receptor was increased in the vessel of the exenatide-treated or rAd-GLP-1-delivered rats compared with the control rats, as in a previous study.[17] Both expression levels increased further in the vessels of the rAd-GLP-1-treated rats.

3.1.1.1 In vivo inhibition of neointimal formation. To determine whether exenatide treatment or rAd-GLP-1 delivery could alter neointimal formation, we measured the IMR in hematoxylin and eosin (H&E)-stained tissue sections of injured arteries. Two weeks after injury, the exenatide + rAd-βGAL and NS + rAd-GLP-1 groups showed a significant reduction in neointimal formation vs. the control group (NS + rAd-βGAL) (*Figure 1*). The rAd-GLP-1-delivered rats showed a greater reduction in neointimal formation than the exenatide-treated rats ($P < 0.05$).

Inhibited Proliferation of RAoSMCs after Exenatide Injection and rAd-GLP-1 Delivery

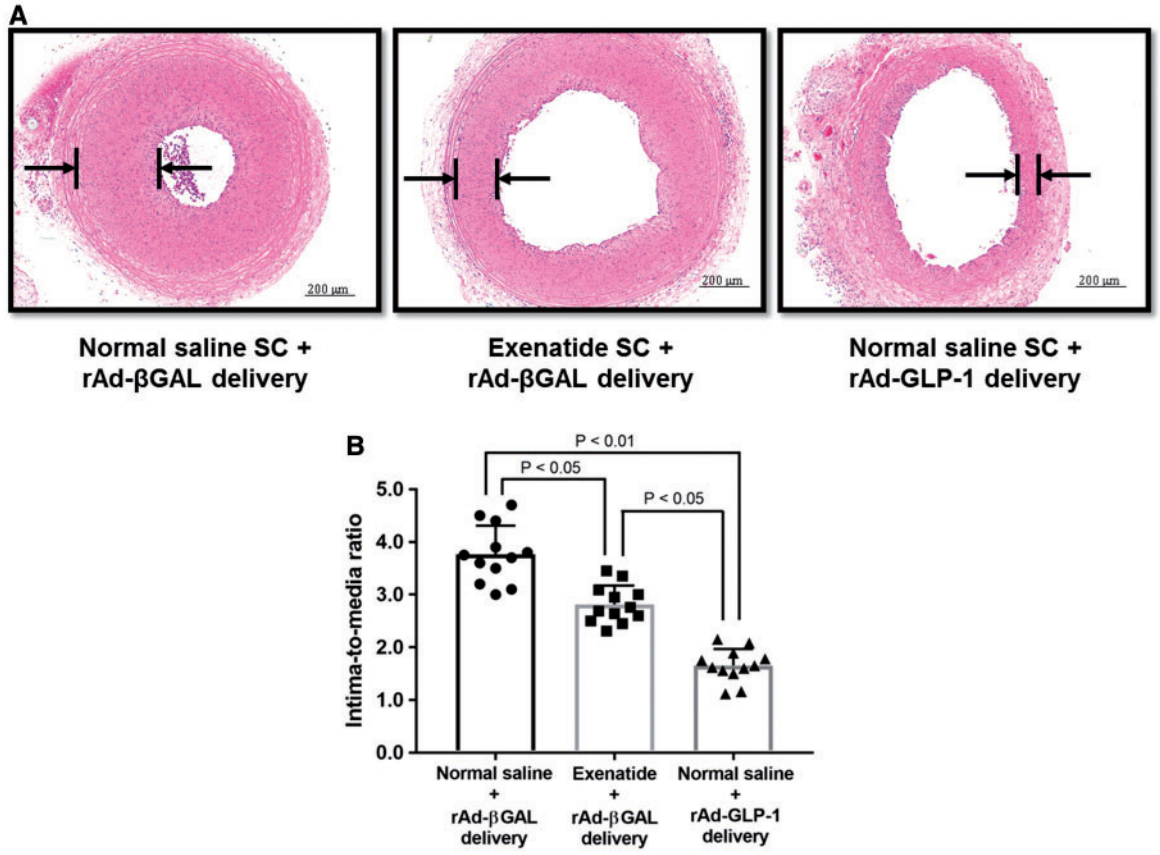

Figure 1 *In vivo* inhibition of neointimal formation after exenatide treatment for 3 weeks (1 week before and 2 weeks after balloon injury) or rAd-GLP-1 delivery at the time of balloon injury. (*A*) H&E stained sections of the three groups (normal saline, NS + rAd-βGAL, exenatide + rAd-βGAL, and NS + rAd-GLP-1). (*B*) Intima-media ratios (IMRs) in the three groups ($n = 12$ in each group). Exenatide injection and rAd-GLP-1 delivery produced a lower IMR than controls, and a lower IMR was found among the rAd-GLP-1-delivered rats compared with exenatide-treated rats ($P < 0.05$).

As shown in *Figure 2*, cell proliferation was markedly lower in the exenatide-treated or rAd-GLP-1-delivered groups than in the controls (open arrow). The rAd-GLP-1 group showed a greater reduction in cell proliferation compared with the exenatide-treated rats ($P < 0.01$).

3.1.2 Sustained apoptosis of vascular cells after exenatide injection or rAd-GLP-1 delivery

Apoptosis of vascular cells was evaluated using TUNEL staining of injured vessels among three groups. After 3 weeks treatment of exenatide or at 2 weeks after balloon injury, the apoptosis index was increased significantly in the exenatide-treated and rAd-GLP-1-delivered groups compared with the control group and further increased in rAd-GLP-1-delivered group compared with the exenatide-treated group ($P < 0.01$) (*Figure 3*).

3.1.1.2 Expression of CD68 and CD31 after exenatide treatment or rAd-GLP-1 delivery. Infiltrations of monocytes stained with CD68 in the neointimal region were decreased in the rAd-GLP-1-delivered and exenatide-treated rats compared with the rAd-βGAL-delivered rats (*Figure 4*). In the injured arteries, endothelial cells stained with CD31 appeared in the injured vessels of the GLP-1-overexpressing and exenatide-treated rats whereas such cells were not observed in the rAd-βGAL-delivered rats (*Figure 5*).

3.1.3 Decreased MMP2 expression after exenatide treatment or rAd-GLP-1 delivery

To clarify whether proliferating smooth muscle cells correspond to the cells expressing MMP2, double staining with an anti-alpha smooth muscle antigen (αSMA) antibody (green) and anti-MMP2 antibody (red) was performed in harvested arteries (*Figure 6*). Cell nuclei were stained with DAPI (blue). The number of cells expressing MMP2 was significantly lower in the control rats than in the exenatide-treated rats ($P < 0.05$). A further decrease was found in the rAd-GLP-1-delivered rats ($P < 0.05$ vs. controls).

3.1.4 Biochemical data associated with cardiovascular risk

Three weeks of treatment of exenatide reduced post-prandial glucose levels at 30 and 60 min significantly, although there was no statistical significance in the reduction of the fasting glucose level (*Table 1*). Glucose tolerance as indicated by the $AUC_{glucose}$ measured in the IPGTT was significantly lower in the exenatide group than in the control or rAd-GLP-1 groups. The HOMA-IR also decreased significantly in the exenatide

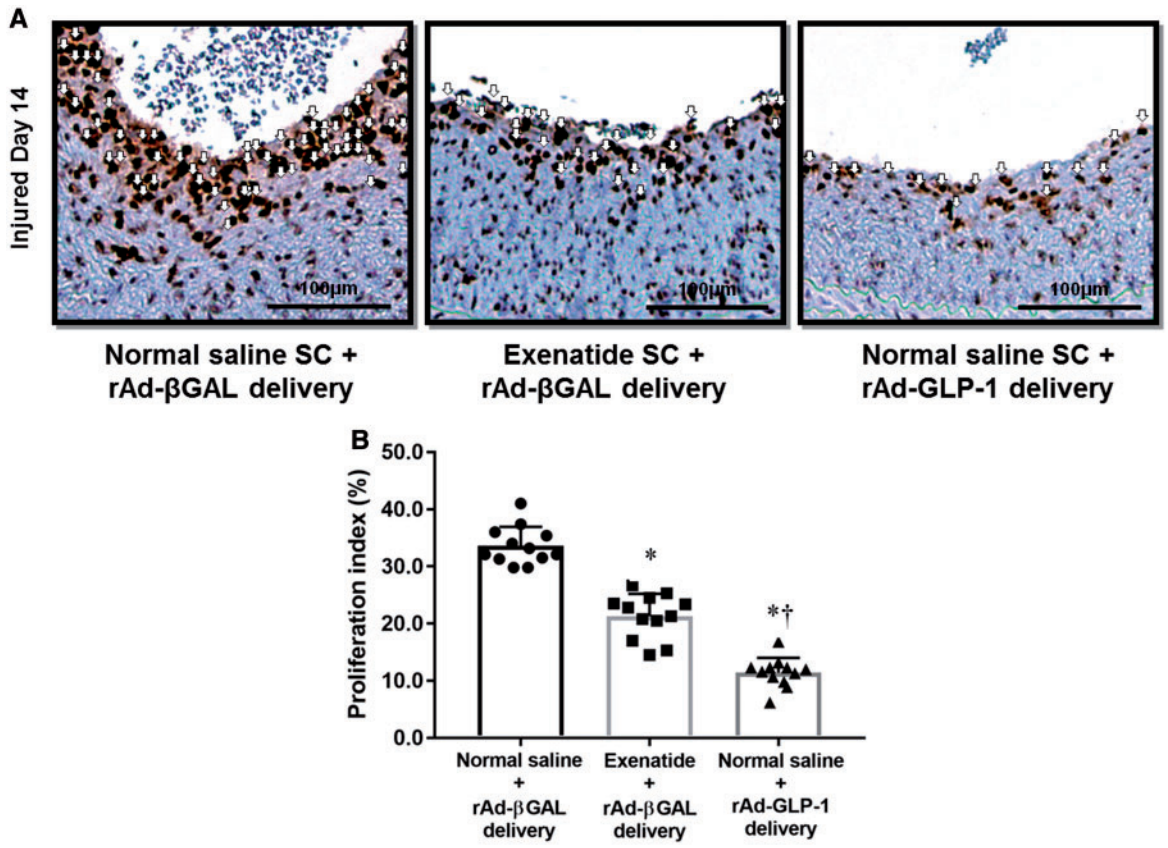

Figure 2 Beneficial effects of rAd-GLP-1 treatment on the proliferation of vascular smooth muscle cells compared with exenatide or normal saline. (*A*) Cell proliferation measured by immunostaining for proliferating cell nuclear antigen (PCNA) was markedly lower in the exenatide-injected and rAd-GLP-1-delivered rats than in the controls (open arrow). (*B*) The proliferation index was significantly different among three groups: control > exenatide-injected rats > rAd-GLP-1-delivered rats (*$P < 0.05$ vs. rAd-βGAL; **$P < 0.05$ between rAd-GLP-1 and exenatide) ($n = 12$ per group).

group compared with the other two groups. HOMA-β did not differ among the three groups.

Treatment with exenatide increased the circulating concentration of adiponectin, which is known to be closely associated with insulin sensitivity. Plasma levels of hsCRP and MCP-1, well known inflammatory markers, were decreased by the exenatide treatment but not in control or rAd-GLP-1 groups (*Table 1*).

3.2 Cell studies

3.2.1 Expression of the GLP-1 receptor in RAoSMCs

In RAoSMCs, exenatide treatment or rAd-GLP-1 delivery increased the expression level of the GLP-1 receptor in time- and dose-dependent manners (see Supplementary material online, *Figure S2*).

3.2.2 RAoSMCs migration and monocyte adhesion in vitro after exenatide or rAd-GLP-1 treatments

Exenatide and rAD-GLP-1 treatments also inhibited the PDGF-BB-directed migration of RAoSMCs (*Figure 7A, B*). TNF-α treatment significantly increased monocyte adhesion in primary rat monocytes, and this was blocked by the treatments with exenatide and delivery of rAd-GLP-1 (*Figure 7C, D*). However, rAd-βGAL delivery did not decrease monocyte adhesion.

3.2.3 Proliferation of RAoSMCs in vitro after exenatide or rAd-GLP-1 treatments

In MTT assays, treatments with exenatide (10 nM) and rAd-GLP-1 (5 and 10 MOIs) inhibited the proliferation in RAoSMCs stimulated with PDGF-BB (see Supplementary material online, *Figure S3*). The proliferation decreased dose-dependently according to the amount of rAd-GLP-1 added.

3.2.4 Expression of p27 and apoptosis in RAoSMCs after exenatide or rAd-GLP-1 treatments

Expression of p27, a cell cycle inhibitor protein, was examined in RAoSMCs. The expression of p27 was decreased by PDGF treatment, but was increased by the treatment with exenatide or rAd-GLP-1, but not by rAd-βGAL (see Supplementary material online, *Figure S4*). Thus, treatment with exenatide and delivery of rAd-GLP-1 delivery inhibited smooth muscle cell proliferation by modulating the cell cycle. When RAoSMCs were incubated with exenatide, the percentage of cells in the sub-G1 phase, indicative of an apoptotic population, was modestly but not significantly increased. In contrast, the sub-G1 population was greatly enriched in GLP-1 overexpressed RAoSMCs (see Supplementary material online, *Figure S5*).

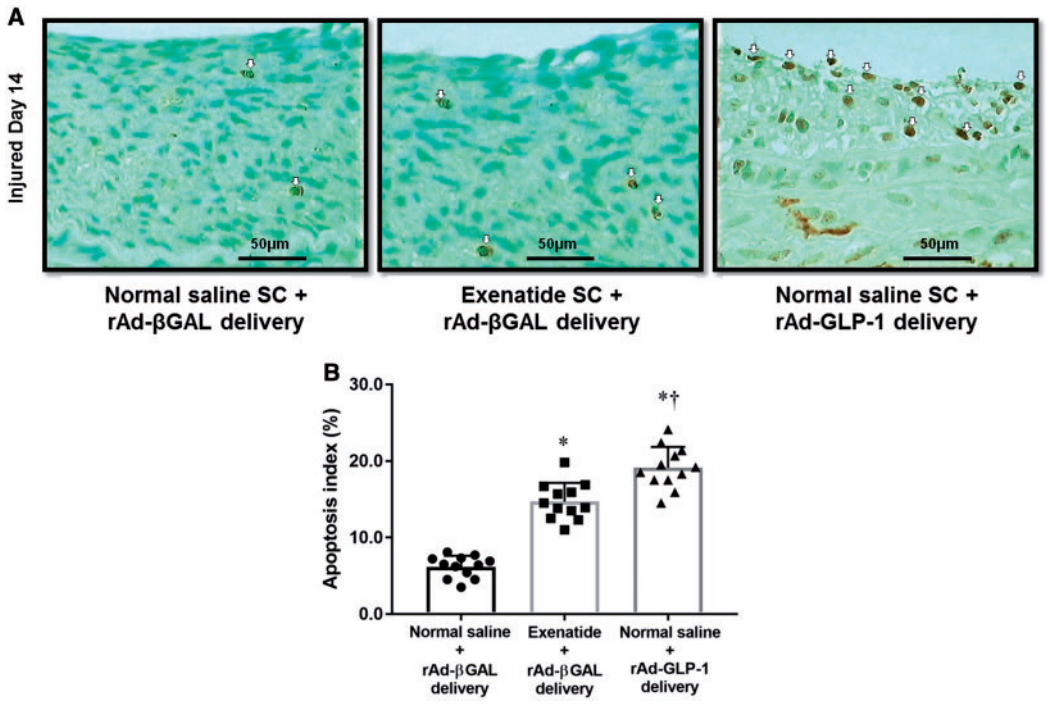

Figure 3 Treatment with rAd-GLP-1 reduced apoptosis of vascular smooth muscle cells compared with exenatide or normal saline. (*A*) TUNEL staining of the three groups (open arrow). (*B*) Apoptosis index (%) at 2 weeks after balloon injury. Apoptosis was significantly higher in the exenatide-treated and rAd-GLP-1-delivered rats than in the control rats, and the index was significantly different among the three groups: control < exenatide-treated rats < rAd-GLP-1-delivered rats (*$P < 0.05$ vs. rAd-βGAL; **$P < 0.05$ between rAd-GLP-1 and exenatide) ($n = 12$ per group).

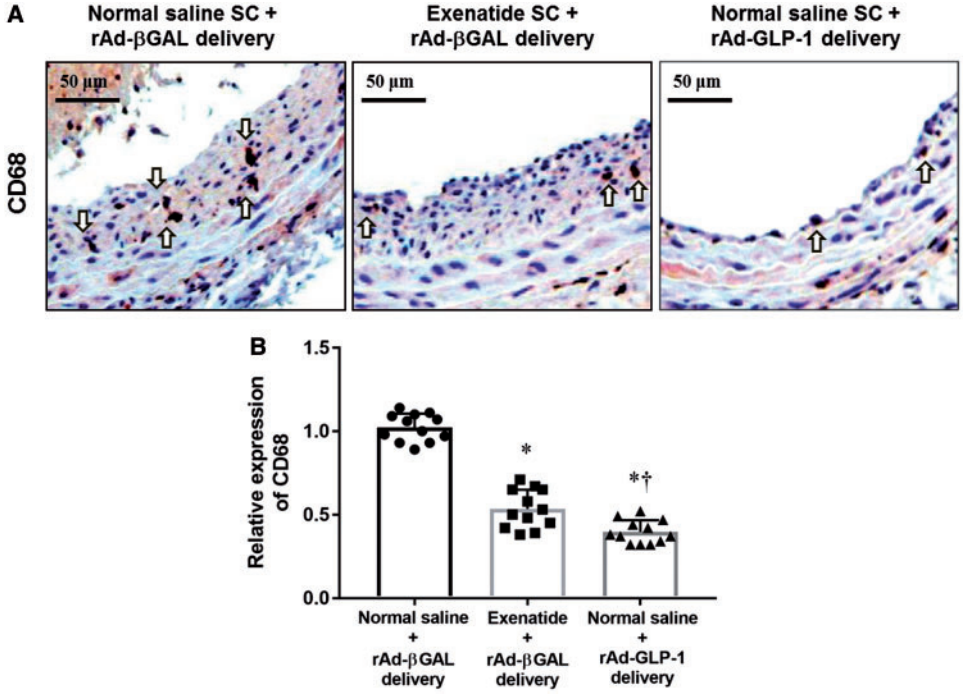

Figure 4 Treatment with rAd-GLP-1 decreased CD68-expressing cells in tissue sections of injured arteries ($n = 12$ per group). Immunofluorescence was used to stain CD68 (*$P < 0.05$ vs. rAd-βGAL; **$P < 0.05$ between rAd-GLP-1 and exenatide).

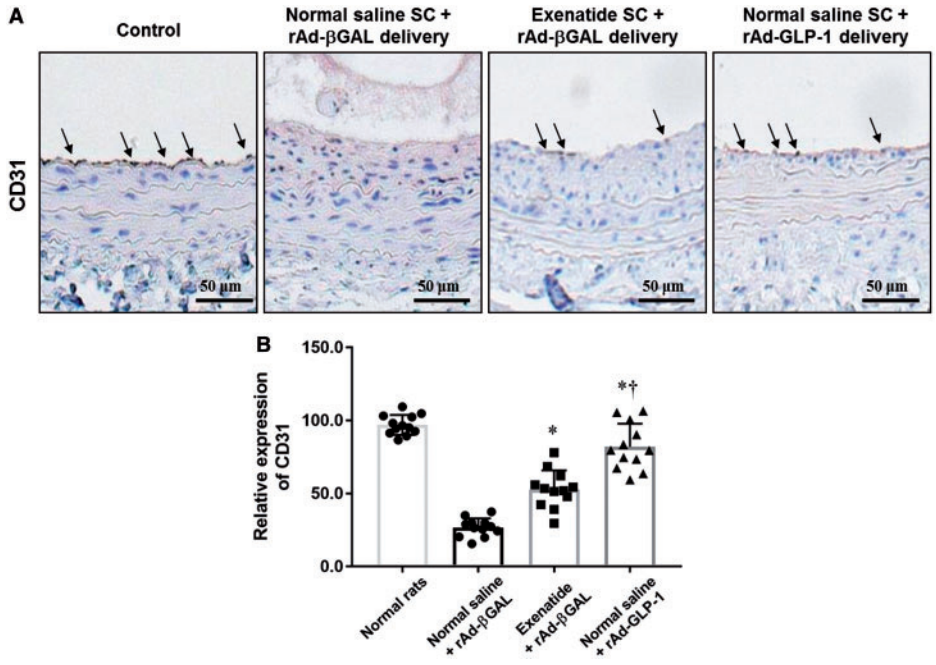

Figure 5 Greater reendothelization in rAd-GLP-1 treatment compared with exenatide or normal saline. Immunofluorescent staining for CD31-expressing cells in tissue sections of injured arteries ($n = 12$ per group) (*$P < 0.05$ vs. rAd-βGAL; **$P < 0.05$ between rAd-GLP-1 and exenatide).

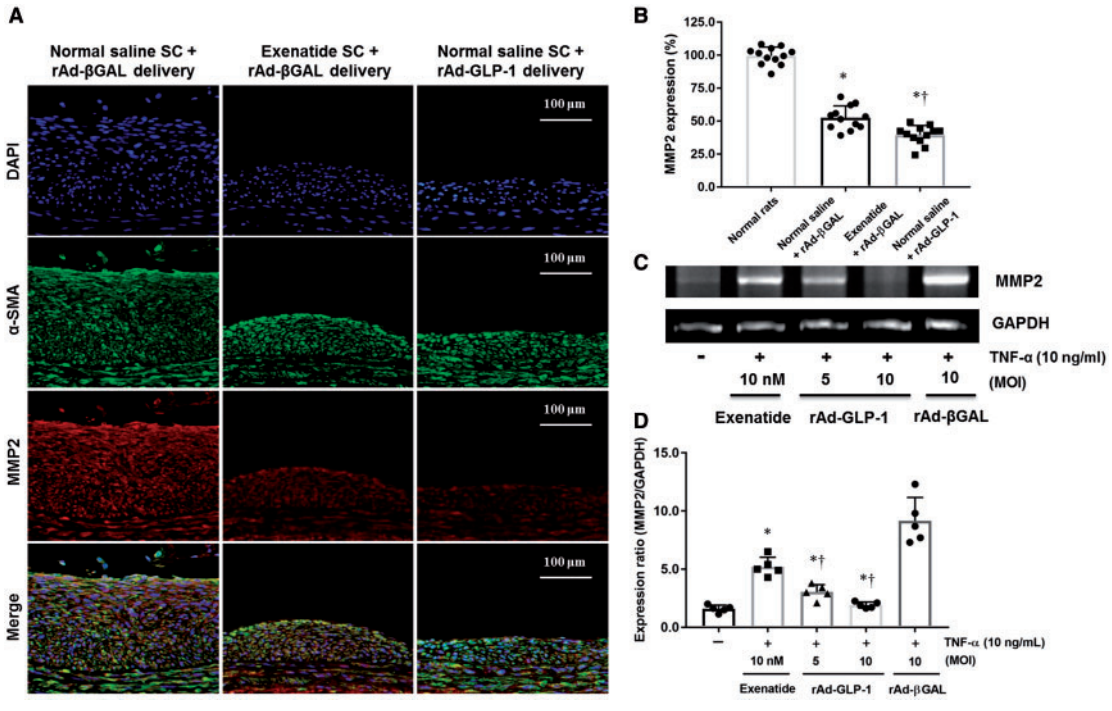

Figure 6 MMP2 Expression in tissue sections of injured arteries and *in vitro* RAoSMCs. (*A* and *B*) Immunofluorescent double staining was done with an anti-αSMA antibody (green) and an anti-MMP2 antibody (red). Nuclei were stained with DAPI (blue) ($n = 12$ per group). (*C* and *D*) *In vitro* effects of exenatide, rAd-GLP-1, and rAd-βGAL virus treatment on MMP2 expression in RAoSMCs ($n = 5$). Delivery of rAd-GLP-1 decreased MMP2 expression in tissue sections of injured arteries and RAoSMCs more than exenatide treatment (*$P < 0.05$ compared with (*$P < 0.05$ vs. rAd-βGAL; **$P < 0.05$ between rAd-GLP-1 and exenatide).

Table 1 Weight and biochemical parameters according to the treatment groups

	Control (normal saline + rAd-βGAL)	Exenatide (exenatide + rAd-βGAL)	rAd-GLP-1 (normal saline + rAd-GLP-1)	*P*[a]	*Post-hoc*[b]
	Mean ± SD	Mean ± SD	Mean ± SD		
Weight (g)	550.0 ± 31.7	534.0 ± 28.8	542.6 ± 31.5	NS	
Fasting glucose (mg/dl)	179.3 ± 43.5	159.2 ± 38.5	170.2 ± 45.3	NS	
Post-load 30 m glucose (mg/dl)	339.9 ± 28.5	301.7 ± 25.7	328.3 ± 29.2	0.041	A,C
Post-load 60 m glucose (mg/dl)	345.2 ± 45.2	314.2 ± 25.4	339.2 ± 34.1	0.023	A,C
Post-load 120 m glucose (mg/dl)	279.1 ± 32.4	264.2 ± 43.9	288.2 ± 42.1	NS	
$AUC_{glucose}$	613.9 ± 74.3	559.2 ± 67.5	605.2 ± 70.1	NS	A,C
Insulin (pg/ml)	5.53 ± 1.12	4.91 ± 1.44	5.30 ± 1.21	NS	
HOMA-IR[c]	2.45 ± 0.12	1.93 ± 0.14	2.23 ± 0.14	0.012	A,C
HOMA-β[c]	17.15 ± 3.51	18.39 ± 4.32	17.83 ± 4.12	NS	
Glucagon (pg/ml)	231.3 ± 16.1	165.2 ± 29.0	218.5 ± 23.0	0.013	A,C
Total cholesterol (mg/dl)	89.2 ± 20.3	82.3 ± 18.2	79.1 ± 18.3	NS	
Triglycerides (mg/dl)	90.5 ± 26.3	78.2 ± 30.2	87.2 ± 23.1	NS	
HDL-cholesterol (mg/dl)	28.2 ± 5.6	29.2 ± 7.5	27.6 ± 7.2	NS	
LDL-cholesterol (mg/dl)	42.1 ± 14.6	38.9 ± 9.2	39.3 ± 8.2	NS	
Adiponectin (μg/ml)	7.9 ± 3.8	10.3 ± 4.7	9.6 ± 2.9	0.026	A,C
HsCRP (mg/l)[c]	0.18 ± 0.08	0.14 ± 0.07	0.17 ± 0.10	0.032	A,C
TNF-α (pg/ml)	5.2 ± 1.9	4.2 ± 1.3	5.4 ± 1.6	NS	
IL-6 (pg/ml)	14.8 ± 6.2	13.2 ± 4.6	15.1 ± 6.9	NS	
MCP-1 (pg/ml)	187.2 ± 37.1	151.5 ± 29.5	172.8 ± 33.9	0.023	A,C

Data are means ± SD. SC, subcutaneous injection, AUC, area under the curve
[a]Statistical significance by one-way analysis of variances among groups.
[b]*Post-hoc* analysis by least significant difference *t*-test (mean difference between two groups: A = control vs. exenatide, B = control vs. rAd-GLP-1, C = exenatide vs. rAd-GLP-1, $P < 0.05$ in all cases).
[c]Log-transformed values were used for comparison.

3.2.5 Effect of exenatide treatment or rAd-GLP-1 delivery on MMP2 expression in RAoSMCs and HUVECs

Exenatide treatment and rAd-GLP-1 delivery reduced MMP2 expression significantly in RAoSMCs (*$P < 0.05$ vs. rAd-βGAL, **$P < 0.05$ vs. exenatide in *Figure 6C, D*). Expression of activated MMP2 in TNF-α treated HUVECs was also decreased significantly with exenatide treatment or delivery of rAd-GLP-1 compared with rAd-βGAL infection ($P < 0.01$) (see Supplementary material online, *Figure S6*).

3.2.6 NF-κB-p65 translocation by exenatide treatment or rAd-GLP-1 infection

Treatment with TNF-α (10 ng/ml) induced translocation of NF-κB-p65 into the nucleus, and this was reduced by exenatide treatment (10 nM) and rAd-GLP-1 delivery (5 and 10 MOIs) (*$P < 0.05$ vs. control, **$P < 0.05$ vs. exenatide in *Figure 8A, B*).

3.2.7 Changes in MCP-1 and VCAM expression levels after GLP-1 treatment

The delivery of rAd-βGAL did not affect increased MCP-1 expression in U937 monocytes or VCAM expression in RAoSMCs induced by TNF-α treatment. The rAd-GLP-1 delivery reduced MCP-1 expression significantly, but the effect of exenatide was modest (*$P < 0.05$ vs. rAd-βGAL, **$P < 0.05$ vs. exenatide in *Figure 8C, D*). Both exenatide treatment and rAd-GLP-1 delivery reduced VCAM expression significantly in RAoSMCs (*$P < 0.05$ vs. rAd-βGAL, in *Figure 8E, F*).

4. Discussion

This study demonstrated that treatment with a systemic injection of exenatide, a GLP-1 agonist, and direct delivery of rAd-GLP-1 to the carotid artery reduced restenosis after balloon injury in this OLETF rat model of obese T2D. *In vivo* and *in vitro* studies showed that rAd-GLP-1 delivery suppressed vascular smooth muscle cell (VSMC) proliferation, promoted VSMC apoptosis, and reduced inflammatory processes more effectively compared with exenatide treatment. Thus, increased GLP-1 activity by direct GLP-1 transduction might have more prominent protective effects against the development of restenosis and possibly atherosclerosis than would systemic GLP-1 agonist administration. This suggests that the local activation of GLP-1 plays an important role in the prevention of restenosis and might be crucial in the prevention of vascular complications in patients with T2D. Previously, it was reported that various cell types including endothelial cells, VSMCs, and cardiomyocytes express a functional GLP-1 receptor.[18] In the present study, the beneficial effect of GLP-1 delivery might have arisen via the GLP-1 receptor because GLP-1 receptor expression was increased by rAd-GLP-1 delivery.

Here, we have demonstrated for the first time direct effects of GLP-1 on the development of restenosis following balloon injury and elucidated its mechanisms using a recombinant adenovirus system. Several studies have already reported the cardioprotective effect of GLP-1 analogues in animal models with heart failure or after acute myocardial infarction.[2–4] These results have been extended to humans; in patients with T2D and coronary artery disease, GLP-1 infusion significantly increased brachial artery diameters modified by flow mediated dilatation by two-fold from

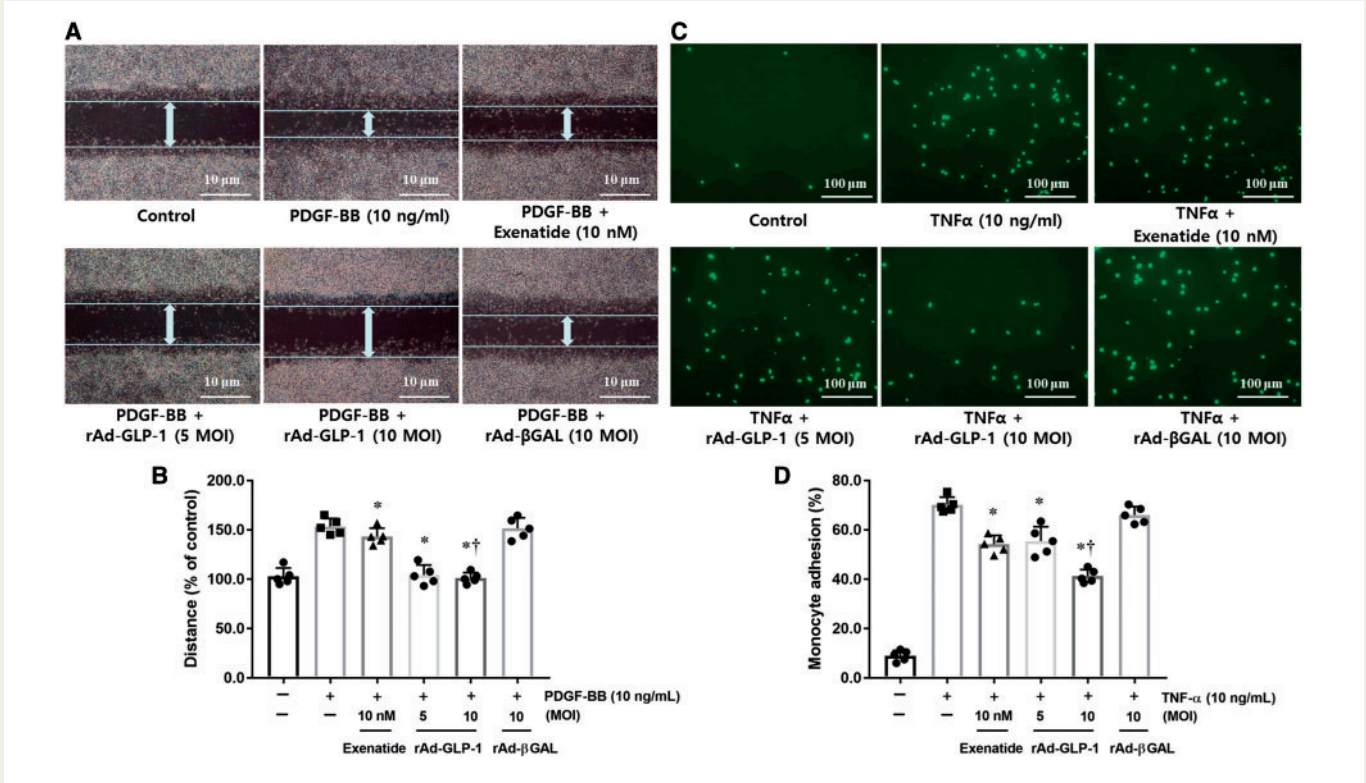

Figure 7 (*A*) Effects of rAd-GLP-1 on the migration of rat aortic smooth muscle cells (RAoSMCs) compared with exenatide (10 nM). (*B*) Dose-dependent inhibiting pattern of PDGF-BB-directed migration after treatment with 5–10 MOI of rAd-GLP-1 in five independent experiments (*$P < 0.05$ compared with PDGF-BB treatment; **$P < 0.05$ compared with exenatide). (*C*) Effects of rAd-GLP-1 and exenatide treatment on TNFα-stimulated monocyte adhesion using isolated rat monocytes. (*D*) Dose-dependent inhibiting pattern of TNFα-stimulated monocyte adhesion after treatment with 5–10 MOI of rAd-GLP-1 in 5 independent experiments (*$P < 0.05$ compared with TNFα treatment; **$P < 0.05$ compared with exenatide).

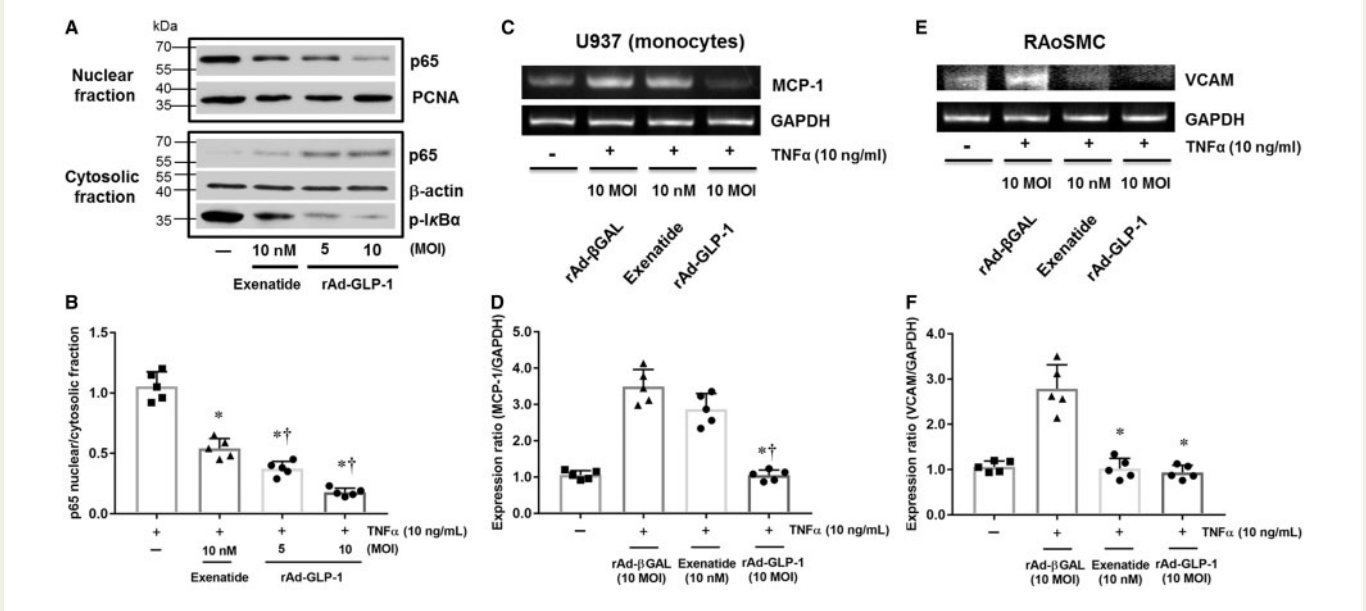

Figure 8 (*A* and *B*) TNF-α-induced NF-κB-p65 translocation into the nucleus in HUVECs was decreased by rAd-GLP-1 treatment, which was greater than exenatide treatment. From both nuclear and cytosolic fractions, western blotting was performed using anti-p65 and anti-phospho-IκB-specific antibodies ($n = 5$). (*C* and *D*) Decrease in MCP-1 expression in U937 cells was more prominent in rAd-GLP-1 treatment compared to exenatide treatment ($n = 5$). (*E* and *F*) VCAM expressions in RAoSMCs were decreased after exenatide and rAd-GLP-1 treatment ($n = 5$) (*$P < 0.05$ vs. control; **$P < 0.05$ between rAd-GLP-1 and exenatide).

baseline.[19] It has also been reported that pre-treatment with the GLP-1 amide (7–36 amino acids) can protect against ischemic left ventricular dysfunction in patients undergoing elective percutaneous coronary intervention.[20] Recently, liraglutide treatment lowered the rate of the first occurrence of death from cardiovascular causes, non-fatal myocardial infarction, or non-fatal stroke among patients with T2D in a large clinical trial.[6] However, there have been no animal or human studies using direct delivery of GLP-1 into culprit vessels.

Several mechanistic experiments were conducted in our study. MMP2 levels were reduced in the target vessels by GLP-1 transduction. MMP2 is well known to play a fundamental role in the migration of VSMCs in general and matrix remodelling during wound healing, and it is produced by VSMCs, endothelial cells, macrophages, lymphocytes, and mast cells in response to mechanical injury.[21] Activated MMPs are able to degrade extracellular molecules including collagen and elastin, resulting in atherosclerotic effects within the arterial wall.[22] Patients with T2D at high risk for acute coronary events have increased levels of MMP2 and an increased propensity of their atherosclerotic plaques to ulceration and thrombosis.[23,24] In fact, significant elevations in MMPs 24 h post-percutaneous coronary intervention was associated with the development of instant restenosis following drug-eluting stent implantation.[25] Thus, reduced MMP2 expression caused by GLP-1 delivery appears to be a key mechanism in preventing vascular restenosis.

In this study, overexpression of GLP-1 in the injured vessels reduced monocyte infiltration and improved reendothelialization, with stronger effects following direct GLP-1 transfection than with systemic exenatide treatment. Such effects also appear to have contributed to a decrease in neointimal formation.[12,26] It is well known that infiltration and adhesion of inflammatory cells occurs early after endothelial denudation.[27–29] Thus, inflammatory and endothelial cells participate in rupture of atherosclerotic plaques.[30] Inhibition of these processes is important in preventing restenosis and mitigating atherosclerosis.[29] In addition, inflammatory and endothelial cells synthesize and secrete MMP2 locally in atherosclerotic lesions.[31] A study on mice fed a high-fat diet showed that treatment with liraglutide (a human GLP-1 analogue; 30 μg/kg twice daily) decreased TNF-α expression and its downstream signalling mediator NF-κB-p65 translocation, and this agent also reduced adhesion of human monocytes to TNF-α-activated human endothelial cells.[32] In our study, the rAd-GLP-1 delivery decreased MMP2 expression *in vivo* and decreased VSMC migration, MMP2 activation, and monocyte adhesion *in vitro*. These results imply that direct transduction of GLP-1 might be more effective in the prevention of restenosis than would the systemic GLP-1 analogue treatment.

In the present study, cardiometabolic benefits were observed along with reduction of neointimal formation after exenatide injection for 3 weeks. Previous studies showed that systemic treatment of GLP-1 agonists produced antirestenotic effects.[33,34] These cardioprotective actions of exenatide seem to be beyond the effects of glucose control and weight loss.[35] Circulating levels of adiponectin, hsCRP, and MCP-1 were altered after the exenatide treatment. MCP-1 has been reported to play an important role in the pathogenesis of atherosclerosis, and evidence suggests that monocytes containing MCPs and macrophages influence the growth of other cell types within atherosclerotic lesions.[36] In the current study, as shown by *in vitro* and *in vivo* experiments, the antirestenotic effect of direct rAd-GLP-1 delivery was greater than that of systemic GLP-1 treatment, indicating that it was independent of the systemic effect of GLP-1 analogue treatment.

In a different context, the direct glucose-lowering effects of exenatide and its weight-reducing tendency might contribute to improvements in glucose tolerance in the exenatide-treated rats although the treatment was only for 3 weeks. Systemic reductions in inflammation and increases in adiponectin concentrations by exenatide treatment are also likely to contribute to this improvement. However, systemic GLP-1 agonist treatments have side effects such as gastrointestinal discomforts. Concern about thyroid cancer has not been clearly resolved. Instead, local treatment has advantages such as fewer systemic side effects and optimizing the effect of GLP-1 to a greater extent than systemic treatment.

In conclusion, the local delivery of rAd-GLP-1 to the culprit vessel had protective properties against the development of restenosis in an animal model of insulin resistance. Decreased MMP2 expression and NF-κB-p65 translocation, as well as a reduction in the proliferation and migration of RAoSMCs were observed.

Our observations provide, for the first time, a potential mechanism for the vascular benefits of a direct increase in GLP-1 activity, suggesting therapeutic implications for treating macrovascular complications in diabetes. These effects were apparently independent of the glucose-lowering effect of incretin-based treatment. Although the feasibility and possible side effects of using a viral vector for increasing GLP-1 levels and preventing atherosclerotic plaque formation warrant further investigations, local activation of GLP-1 might have vasculoprotective effects in a milieu of insulin resistance and atherosclerosis.

Supplementary material

Supplementary material is available at *Cardiovascular Research* online.

Funding

This work was supported by research grant from the Seoul National University Bundang Hospital (14-2015-014) and Korean Diabetes Association (06-2014-260).

Conflict of interest: none declared.

References

1. Rodriguez AE, Maree AO, Mieres J, Berrocal D, Grinfeld L, Fernandez-Pereira C, Curotto V, Rodriguez-Granillo A, O'Neill W, Palacios IF. Late loss of early benefit from drug-eluting stents when compared with bare-metal stents and coronary artery bypass surgery: 3 years follow-up of the ERACI III registry. *Eur Heart J* 2007;**28**:2118–2125.
2. Liu Q, Anderson C, Broyde A, Polizzi C, Fernandez R, Baron A, Parkes DG. Glucagon-like peptide-1 and the exenatide analogue AC3174 improve cardiac function, cardiac remodeling, and survival in rats with chronic heart failure. *Cardiovasc Diabetol* 2010;**9**:76.
3. Zhao T, Parikh P, Bhashyam S, Bolukoglu H, Poornima I, Shen YT, Shannon RP. Direct effects of glucagon-like peptide-1 on myocardial contractility and glucose uptake in normal and postischemic isolated rat hearts. *J Pharmacol Exp Ther* 2006;**317**:1106–1113.
4. Nikolaidis LA, Elahi D, Shen YT, Shannon RP. Active metabolite of GLP-1 mediates myocardial glucose uptake and improves left ventricular performance in conscious dogs with dilated cardiomyopathy. *Am J Physiol Heart Circ Physiol* 2005;**289**:H2401–2408.
5. Sokos GG, Bolukoglu H, German J, Hentosz T, Magovern GJ Jr, Maher TD, Dean DA, Bailey SH, Marrone G, Benckart DH, Elahi D, Shannon RP. Effect of glucagon-like peptide-1 (GLP-1) on glycemic control and left ventricular function in patients undergoing coronary artery bypass grafting. *Am J Cardiol* 2007;**100**:824–829.
6. Marso SP, Daniels GH, Brown-Frandsen K, Kristensen P, Mann JF, Nauck MA, Nissen SE, Pocock S, Poulter NR, Ravn LS, Steinberg WM, Stockner M, Zinman B, Bergenstal RM, Buse JB, Investigators LSCobotLT. Liraglutide and cardiovascular outcomes in Type 2 diabetes. *N Engl J Med* 2016;**375**:311–322.
7. Liu MJ, Shin S, Li N, Shigihara T, Lee YS, Yoon JW, Jun HS. Prolonged remission of diabetes by regeneration of beta cells in diabetic mice treated with recombinant adenoviral vector expressing glucagon-like peptide-1. *Mol Ther* 2007;**15**:86–93.
8. Marx N, Froehlich J, Siam L, Ittner J, Wierse G, Schmidt A, Scharnagl H, Hombach V, Koenig W. Antidiabetic PPAR gamma-activator rosiglitazone reduces MMP-9 serum

levels in type 2 diabetic patients with coronary artery disease. *Arterioscler Thromb Vasc Biol* 2003;**23**:283–288.
9. Maxwell PR, Timms PM, Chandran S, Gordon D. Peripheral blood level alterations of TIMP-1, MMP-2 and MMP-9 in patients with type 1 diabetes. *Diabet Med* 2001;**18**:777–780.
10. Okitsu T, Kobayashi N, Jun HS, Shin S, Kim SJ, Han J, Kwon H, Sakaguchi M, Totsugawa T, Kohara M, Westerman KA, Tanaka N, Leboulch P, Yoon JW. Transplantation of reversibly immortalized insulin-secreting human hepatocytes controls diabetes in pancreatectomized pigs. *Diabetes* 2004;**53**:105–112.
11. Yu Y, Ohmori K, Chen Y, Sato C, Kiyomoto H, Shinomiya K, Takeuchi H, Mizushige K, Kohno M. Effects of pravastatin on progression of glucose intolerance and cardiovascular remodeling in a type II diabetes model. *J Am Coll Cardiol* 2004;**44**:904–913.
12. Lim S, Moon MK, Shin H, Kim TH, Cho BJ, Kim M, Park HS, Choi SH, Ko SH, Chung MH, Lee IK, Jang HC, Kim YB, Park KS. Effect of S-adenosylmethionine on neointimal formation after balloon injury in obese diabetic rats. *Cardiovasc Res* 2011;**90**:383–393.
13. Lim S, Jin CJ, Kim M, Chung SS, Park HS, Lee IK, Lee CT, Cho YM, Lee HK, Park KS. PPARgamma gene transfer sustains apoptosis, inhibits vascular smooth muscle cell proliferation, and reduces neointima formation after balloon injury in rats. *Arterioscler Thromb Vasc Biol* 2006;**26**:808–813.
14. Ansari B, Coates PJ, Greenstein BD, Hall PA. In situ end-labelling detects DNA strand breaks in apoptosis and other physiological and pathological states. *J Pathol* 1993;**170**:1–8.
15. Matthews DR, Hosker JP, Rudenski AS, Naylor BA, Treacher DF, Turner RC. Homeostasis model assessment: insulin resistance and beta-cell function from fasting plasma glucose and insulin concentrations in man. *Diabetologia* 1985;**28**:412–419.
16. Posel C, Moller K, Frohlich W, Schulz I, Boltze J, Wagner DC. Density gradient centrifugation compromises bone marrow mononuclear cell yield. *PLoS One* 2012;**7**:e50293.
17. Poornima I, Brown SB, Bhashyam S, Parikh P, Bolukoglu H, Shannon RP. Chronic glucagon-like peptide-1 infusion sustains left ventricular systolic function and prolongs survival in the spontaneously hypertensive, heart failure-prone rat. *Circ Heart Fail* 2008;**1**:153–160.
18. Ban K, Noyan-Ashraf MH, Hoefer J, Bolz SS, Drucker DJ, Husain M. Cardioprotective and vasodilatory actions of glucagon-like peptide 1 receptor are mediated through both glucagon-like peptide 1 receptor-dependent and -independent pathways. *Circulation* 2008;**117**:2340–2350.
19. Nystrom T, Gutniak MK, Zhang Q, Zhang F, Holst JJ, Ahren B, Sjoholm A. Effects of glucagon-like peptide-1 on endothelial function in type 2 diabetes patients with stable coronary artery disease. *Am J Physiol Endocrinol Metab* 2004;**287**:E1209–1215.
20. McCormick LM, Hoole SP, White PA, Read PA, Axell RG, Clarke SJ, O'Sullivan M, West NE, Dutka DP. Pre-treatment with glucagon-like Peptide-1 protects against ischemic left ventricular dysfunction and stunning without a detected difference in myocardial substrate utilization. *JACC Cardiovasc Interv* 2015;**8**:292–301.
21. Wang M, Kim SH, Monticone RE, Lakatta EG. Matrix metalloproteinases promote arterial remodeling in aging, hypertension, and atherosclerosis. *Hypertension* 2015;**65**:698–703.
22. Lakatta EG. The reality of aging viewed from the arterial wall. *Artery Res* 2013;**7**:73–80.
23. Cooper ME, Bonnet F, Oldfield M, Jandeleit-Dahm K. Mechanisms of diabetic vasculopathy: an overview. *Am J Hypertens* 2001;**14**:475–486.
24. Derosa G, D'Angelo A, Tinelli C, Devangelio E, Consoli A, Miccoli R, Penno G, Del Prato S, Paniga S, Cicero AF. Evaluation of metalloproteinase 2 and 9 levels and their inhibitors in diabetic and healthy subjects. *Diabetes Metab* 2007;**33**:129–134.
25. Tarr GP, Williams MJ, Wilkins GT, Chen VH, Phillips LV, van Rij AM, Jones GT. Intra-individual changes of active matrix metalloproteinase-9 are associated with clinical in-stent restenosis of bare metal stents. *Cardiology* 2013;**124**:28–35.
26. Gutierrez G, Mendoza C, Zapata E, Montiel A, Reyes E, Montano LF, Lopez-Marure R. Dehydroepiandrosterone inhibits the TNF-alpha-induced inflammatory response in human umbilical vein endothelial cells. *Atherosclerosis* 2007;**190**:90–99.
27. Moreno PR, Fallon JT, Murcia AM, Leon MN, Simosa H, Fuster V, Palacios IF. Tissue characteristics of restenosis after percutaneous transluminal coronary angioplasty in diabetic patients. *J Am Coll Cardiol* 1999;**34**:1045–1049.
28. Rogers C, Welt FG, Karnovsky MJ, Edelman ER. Monocyte recruitment and neointimal hyperplasia in rabbits. Coupled inhibitory effects of heparin. *Arterioscler Thromb Vasc Biol* 1996;**16**:1312–1318.
29. Welt FG, Edelman ER, Simon DI, Rogers C. Neutrophil, not macrophage, infiltration precedes neointimal thickening in balloon-injured arteries. *Arterioscler Thromb Vasc Biol* 2000;**20**:2553–2558.
30. Galis ZS, Sukhova GK, Lark MW, Libby P. Increased expression of matrix metalloproteinases and matrix degrading activity in vulnerable regions of human atherosclerotic plaques. *J Clin Invest* 1994;**94**:2493–2503.
31. Falk E, Shah PK, Fuster V. Coronary plaque disruption. *Circulation* 1995;**92**:657–671.
32. Noyan-Ashraf MH, Shikatani EA, Schuiki I, Mukovozov I, Wu J, Li RK, Volchuk A, Robinson LA, Billia F, Drucker DJ, Husain M. A glucagon-like peptide-1 analog reverses the molecular pathology and cardiac dysfunction of a mouse model of obesity. *Circulation* 2013;**127**:74–85.
33. Goto H, Nomiyama T, Mita T, Yasunari E, Azuma K, Komiya K, Arakawa M, Jin WL, Kanazawa A, Kawamori R, Fujitani Y, Hirose T, Watada H. Exendin-4, a glucagon-like peptide-1 receptor agonist, reduces intimal thickening after vascular injury. *Biochem Biophys Res Commun* 2011;**405**:79–84.
34. Hirata Y, Kurobe H, Nishio C, Tanaka K, Fukuda D, Uematsu E, Nishimoto S, Soeki T, Harada N, Sakaue H, Kitagawa T, Shimabukuro M, Nakaya Y, Sata M. Exendin-4, a glucagon-like peptide-1 receptor agonist, attenuates neointimal hyperplasia after vascular injury. *Eur J Pharmacol* 2013;**699**:106–111.
35. Yoon JS, Lee HW. Understanding the cardiovascular effects of incretin. *Diabetes Metab J* 2011;**35**:437–443.
36. Lin J, Kakkar V, Lu X. Impact of MCP-1 in atherosclerosis. *Curr Pharm Des* 2014;**20**:4580–4588.